A new generation of silicon solar cells with ultrahigh efficiency

Z.T. Kuznicki

CNRS, Laboratoire PHASE (UPR no 292),
BP 20, 67037 Strasbourg, CEDEX 2, France

1. Introduction

Solar energy conversion into electric current can be obtained directly in semiconductor devices called solar cells. The useful solar spectrum lies between light wavelength of $\lambda \approx 250$ nm up to $\lambda \approx 3200$ nm. Figs. 1 and 2 show solar spectra for different atmospheric conditions in the form of energy density (Fig. 1) and photon flux (Fig. 2). Only a relatively small part of this spectrum can be converted by existing solar cells.

For example, single-crystal single junction silicon solar cells, which are the most used in terrestrial installations, cannot exploit two relatively important parts of the solar spectrum (see Fig. 1). The first fundamental limitation concerns the infrared end of spectrum where photon quantum energies are below the silicon optical bandgap E_{gSi} = 1.12 eV (corresponding to wavelengths $\lambda \geqslant 1100$ nm). These numerous infrared photons (Fig. 2) can be utilized only by thermal conversion in other devices. The second fundamental limitation is related to the effect of only one electron-hole pair generation per energetic photon of UV and visible light. The excess photon energy $\Delta E = E(h\nu) - E_{gSi}$ is transformed into heat. So the energy of these photons can be only partially transformed into electric current. We conclude that in the case of silicon solar cells, which are the only kind mass produced today, there are the two considerable photovoltaic conversion losses:

i) because of too small single photon energies – a fraction of the solar energy comparable to that converted is lost for electron-hole pair generation (such infrared photons are more numerous than visible ones),

ii) because of the photogeneration mechanism – only one electron-hole pair can be created per absorbed photon (again the energy lost is comparable to that converted).

The state of the art of photovoltaic conversion is presented in several review papers as for example [1 ÷ 3]. At the present time both silicon single phase solar cells have attained separately their maximum efficiency performance. Since the early 1980s practical photovoltaic conversion efficiency has progressed very slowly, saturating at 14 ÷ 15% for single-crystals and at 8% for amorphous material.

There are several new concepts concerning other semiconductor materials (elemental and compound) and other device structures which allow a better (sometimes much better) conversion efficiency $\eta \approx 25\%$. But these improvements are made at the expense of device application, technology step multiplication or ecological limits and finally by greater costs. For example, the best actual space solar cells on GaAs with a gradual band-gap can attain a conversion efficiency .Their terrestrial application is not possible because of many reasons (technological, economic and 3 environmental). On the other hand, cells with the best efficiencies, possible with tandem or modulated band-gap devices, are not suitable for practical applications on a really large scale such as terrestrial solar power-stations.

The recent theoretical modeling and numerical simulation of a novel silicon device [4 ÷ 6] show that in the case of a new solar cell founded on the single-crystal material with local modifications, the conversion efficiency can attain 35 ÷ 40% in a single junction device with non-concentrated light. Even in practice, where the real value can be 10 ÷ 15% less, the gain will still be important enough to justify a large effort for conception, development, design and fabrication of the new generation solar cells.

The future fabrication will necessitate uniting recent technological advances in the same fine sub-structure inserted within the single-crystal cell to ensure: i) absorption of low energy photons, ii) corresponding optical confinement of the infrared light, iii) formation of L-H type interfaces at the sub-structure edges, iv) better thermodynamic exploitation of UV and visible photons, v) conditions for new electronic transport properties, and so on.

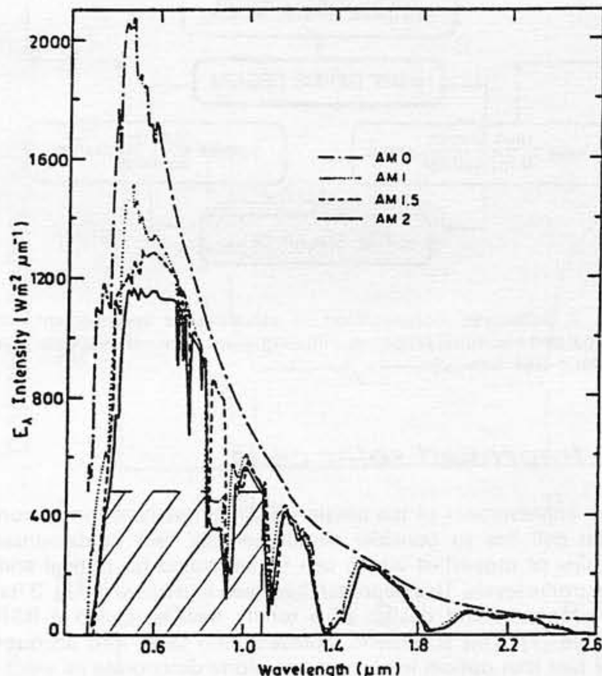

Fig. 1. Solar spectra for different atmospheric conditions in the form of energy density. The photovoltaic conversion area for the silicon single-crystal single-junction is indicated as the hatched area

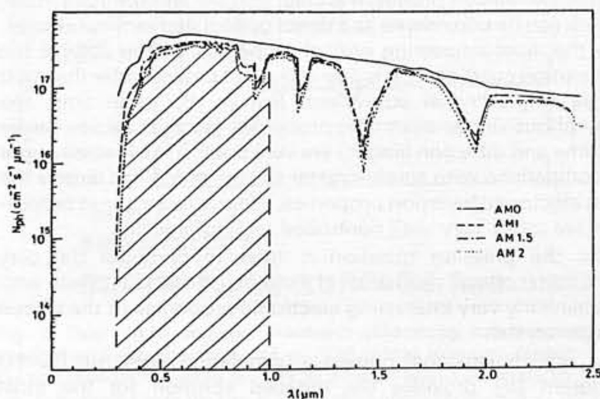

Fig. 2. Solar spectrum photon flux distribution as a function of the light wavelength. The part of the spectrum with photons of sufficient energy to generate electron-hole pairs in a single-crystal silicon device is indicated by the hatched area

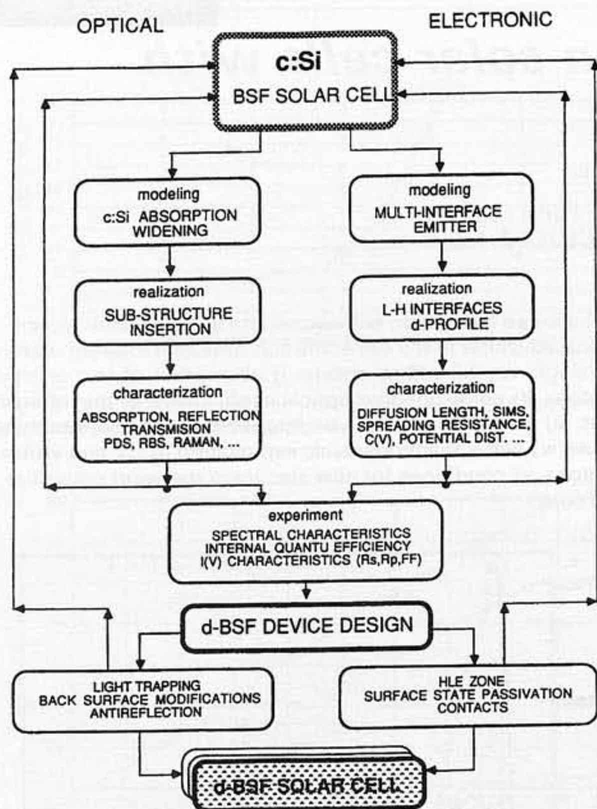

Fig. 3. Schematic representation of simultaneous improvements of optical and electronic properties initiating a new generation of solar cell of the δ-BSF type [7]

2. Improved solar cells

Any improvement of the single-crystal single junction silicon solar cell has to consider simultaneously two fundamental groups of properties which can be separated on optical and electronic levels. This approach has been illustrated in Fig. 3 for development and design of a totally new so-called δ-BSF device [7]. This schematic representation takes into account the fact that optical improvements alone deteriorate its electronic counterpart, and vice versa.

An interesting example can be cited using the useful property combination of two phases of the same semiconductor material as in the silicon case: single-crystal and amorphous. Fig. 4 shows experimental absorption coefficient results obtained for the two silicon phases. It is clear that the amorphous silicon, which can be considered as a direct optical gap semiconductor, has the most interesting optical properties. In the case of the absorption coefficient, it is one and a half orders better than that of its single-crystal equivalent. But at the same time, the amorphous silicon electronic properties (such as excess carrier lifetime and diffusion length) are very poor. It is especially poor in comparison with single-crystal silicon which has largely the best electronic transport properties. What is more, these properties are today very well controlled technologically.

So the pressing question is how to combine the very interesting optical properties of a silicon amorphous phase with the similarly very interesting electronic properties of the silicon single-crystal.

A one-dimensional numerical simulation with the PC-1D program [9] provides the detailed solution for the most important distributions such as built-in electric fields for the multi-interface device. The modeling and numerical solutions provide physical insight and hence facilitate design ptimization of the one-dimensional L-H interface morphology of the solar cell. Fig. 5 shows the comparison of both built-in electric fields:

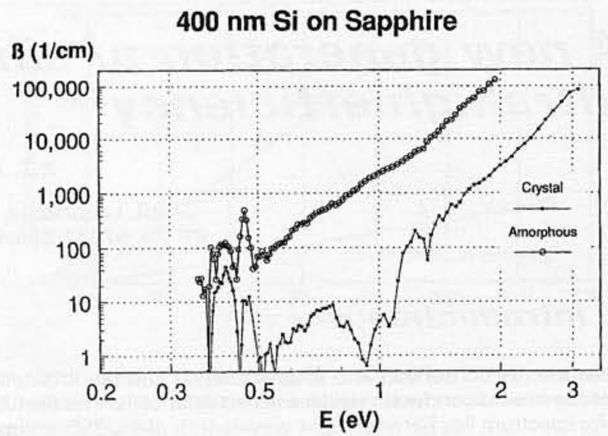

Fig. 4. Experimental absorption coefficients for amorphous and single-crystal silicon obtained by photothermal deflection spectroscopy (PDS). The infrared amorphous silicon absorption is well-visualized [8]

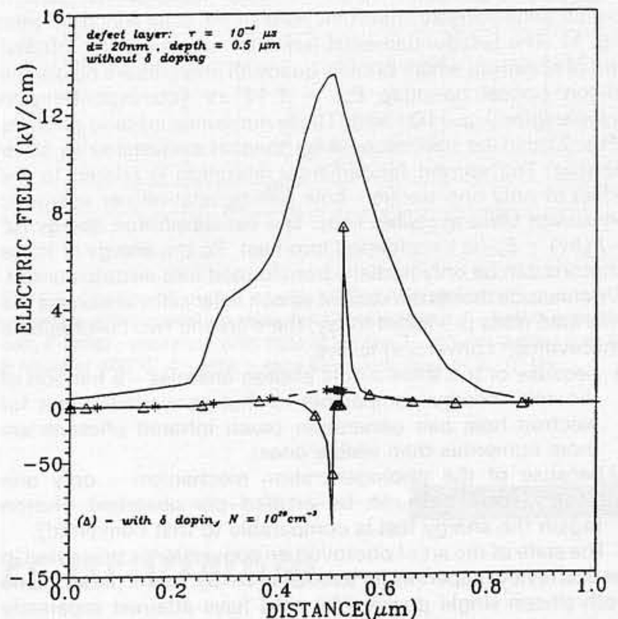

Fig. 5. Electric field distributions within the sub-structure without (*) and with (Δ) δ-doping properties. The assumed sub-structure lifetime is $\tau=10^{-4}$ μs. The sub-structure of 20 nm width is placed at the *p-n* junction interface (x = 0.5 μm) on the base side [4-6]

of the collecting P-N junction and of the inserted L-H interfaces [4 ÷ 6]. It is clear that a relatively important built-in electric field is present at the edges of the inserted -doping sub-structure. These results illustrate only one of the multiple improvements obtained by the L-H type interface insertion. The end result is a totally changed electronic minority carrier behavior inside the emitter by their effective separation from recombination centers.

3. Silicon modifications

It is clear that the silicon based design and technology is the most desired one for solar applications because of the above-mentioned shortcomings of compound semiconductor or multi junction (tandem) structures. Since silicon-based progress has reached a plateau, only new concepts taking into account new phenomena can allow an issue from the present fifteen year old impasse. The most interesting improvement

seems to be possible by uniting optical-amorphous and electronic-single-crystal properties in the simplest possible design. Indeed, this idea has been known since the 1970s but the desired superimposition of properties did not seem not feasible because of contradictions between the optical and electronic improvements.

Optical properties of amorphized silicon. Some interesting optical properties as the long wavelength absorption have been observed in *defected thin structures* [10,11], i.e. in structures having a non-standard monocrystalline (or other) structural arrangement [12÷15]. The sub-structure inserted in the silicon single-crystal could of course be formed from an another semiconductor material [11,16,17].

The addition of optical confinement properties [18] to the modified device can considerably improve its conversion performance because of an increased effective optical length. However, the electron-hole generation by light in defected structures is normally matched by a short lifetime of the generated minority carriers which have too short a *diffusion length* to reach the contact or the silicon *crystalline structure*. The *defected thin structure* can improve the *short-circuit current* I_{sc} but degrades the *open-circuit voltage* V_{oc} by increasing the *saturation current density* [19,11]. Unfortunately the local strong doping provokes another undesired effect, namely a high impurity state concentration within the band-gap which usually shortens the lifetime of the photoexcited carriers so much that no significant increase in photocurrent can be observed. The good single-crystal carrier lifetime (concerning equilibrium and excess carriers) is deteriorated considerably by the large recombination velocity in amorphized material. So a partial silicon amorphization improves significantly the optical absorption but deteriorates simultaneously the initial good device performance because of a recombination zone related to the amorphized region.

Good single-crystal silicon material has a large carrier diffusion length which means that the inserted new property takes the form of a long range phenomenon. Overall performance may be worsened by a simple superimposition of the two geometrically separate phenomena. This example illustrates well the paradoxes in a complex solar cell device.

A new concept which allows to overcome these difficulties is founded upon fundamental device modification, i.e. semiconductor interface insertions. As shown in Fig. 6 the model superimposition of absorption coefficients for silicon single-crystal and modified (amorphous, amorphized) materials gives an interesting absorption widening in the infrared range. The modeling, which preceded experimental realization [20, 21], furnished a necessary estimation of the minimal improvement still being interesting for application. A new material was founded on silicon single-crystal local modification taking the form of a buried nanostructure [7].

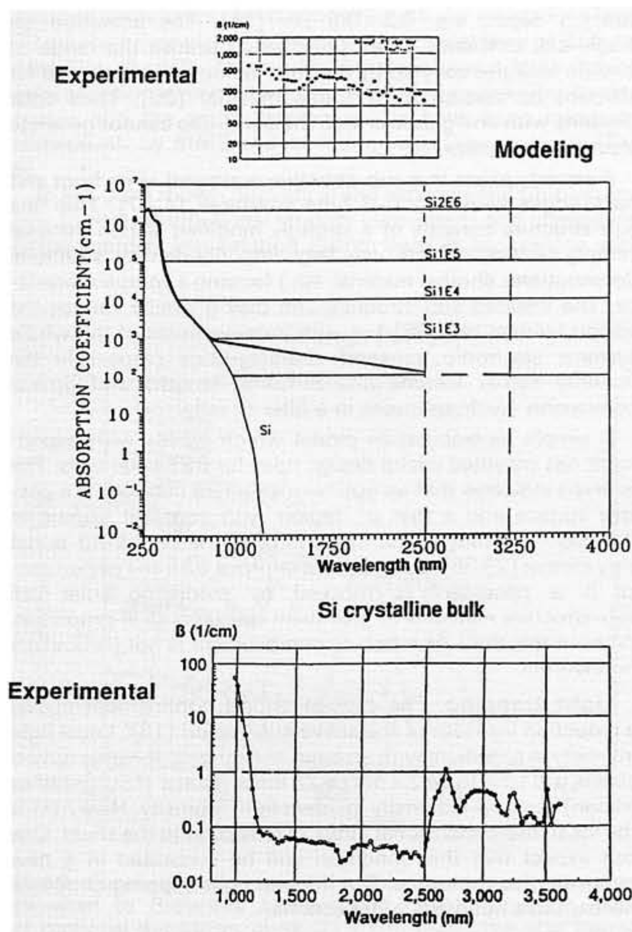

Fig. 6. Superimposition of absorption coefficients for silicon single-crystal and modified (amorphous, amorphized) materials: comparison of model and experimental results. Experimental results have been obtained on implanted silicon wafers by PDS [7,20,21]

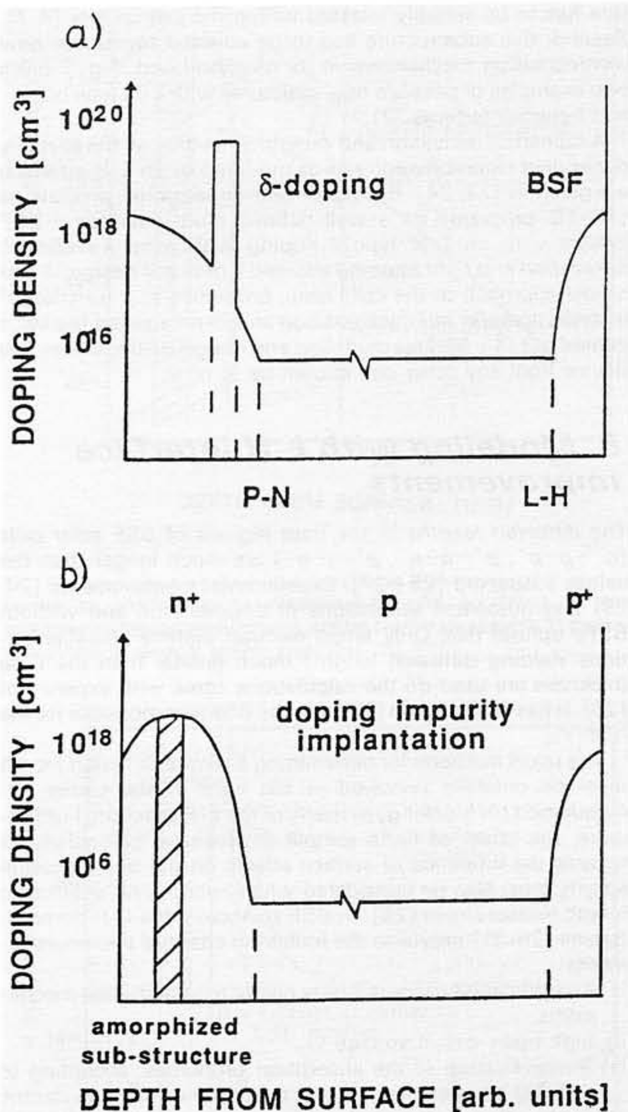

Fig. 7. Two model *complex interfaces* (absorbing sub-structure) in equilibrium inside the emitter of a δ-BSF silicon solar cell illustrated by the two schematic doping profiles: a) a model with a δ-doping ($N=10^{20}$ cm^{-3}) coincides with the two sub-structure positions at $x = 0.21$ μm and $x = 0.50$ μm; the emitter doping n^+ – profile is of the erfc type with the edge surface concentration $N_s = 10^{19}$ cm^{-3}; the sub-structure width is d_i = 20 nm and the total cell thickness is $d_c = 5 \div 200$ μm, b) an experimental realization by phosphorus implantation and conjugated thermal treatment [7,20,21]

4. Multi-interface device: δ-BSF solar cell

Multiple improvements in back surface field (BSF) silicon cells in the 1980s have brought their efficiency up to $20 \div 24\%$. In order to improve the performance of classical single junction high efficiency cells, several solutions have been proposed for advanced structure configurations [$1 \div 3$, 10]. The first aspect consists in semiconductor material modifications so as to increase the minority carrier lifetime by the neutralization of bulk recombination centers by gettering and hydrogenation of defects and impurities. The second aspect concerns optical device characteristics by the creation of minority carrier mirrors (on both the *front* and *back* boundaries of only the active region or of the whole device). The third aspect concerns the device structure by incorporation of the internal substructures as defect layer with L-H type interfaces (δ-doping) and an L-H interface for BSF improvement [22].

Now, several known phenomena normally considered separately have to be taken into account simultaneously to model before, and to realize after, a new generation solar cell family based on silicon material. First, an absorbing planar substructure has to be suitably inserted within the cell emitter [4-7]. Second, this substructure has to be adapted to assume new recombination mechanisms in its neighborhood. Fig. 7 gives two examples of possible new structures with L-H type homo– and hetero-interfaces [7].

A numerical derivation and experimental data on the spatially dependent recombination rate as modified by an L-H interface are given in [23, 24]. Results of one-dimensional simulations (PC-1D program) on a well-defined multi-interface δ-BSF system with an L-H type δ-doping with *long wavelength absorption* and *light trapping* allowed a new cell design. A first model approach to the cells basic properties as a function of inserted *complex* interface position and its parameters has been carried out [$4 \div 6$]. This modeling and design distinguishes this device from any other one known up to now.

5. Modeling with L-H interface improvements

The *diffusion lengths* in the base regions of BSF solar cells (n^+-p-p^+, p^+-n-n^+, p^+-i-n^+) are much longer than the values suspected [$25 \div 27$]. Experimental measurements [24, 28] and numerical simulations of devices with and without BSFs uphold this. Only when electron lifetime characterizations yielding diffusion lengths much greater than the base thickness are used do the calculations agree with experiment [25]. It has been shown [22] that the BSF is responsible for the high V_{oc}.

The usual methods for determining a device diffusion length must be critically reviewed in the light of the carrier accumulation (or blocking) property of the L-H junction. Furthermore, the effect of finite sample dimensions, particularly as regards the influence of surface effects on the bulk diffusion length, must also be considered when interpreting a diffusion length measurement [26]. In BSF solar cells, the L-H homointerface [29-31] provokes the following changes and improvements:

i) a modification of the minority carrier recombination mechanisms,
ii) high open-circuit voltage V_{oc},
iii) a modification of the absorption properties: according to [32,33] it has to be noted that the presence of a thin electric field region at the back surface of a cell could produce significant increases in long-wavelength response,
iv) the creation of a built-in electric field playing the role of an electrical mirror for the minority carriers,
v) a modification of the geometrical factors of the device and a decrease of structure thickness (lightweight structures for space solar cells),
vi) a modification of the band model in the heavily doped region [34],
vii) the creation of sub-regions in the base having different characteristic lengths near the structural homointerface (depletion and accumulation layers as well as weak and strong built-in electric field regions within the accumulation layer [29]).

These properties are of interest for new concept high efficiency silicon cells where a thin sub-structure as a complex interface (with δ-doping profile) can be buried in the emitter The improvement is possible in spite of a large impurity concentration by a substantial reduction of the highly doped layer thickness and by a slowing down of recombination velocities with the appearance of accumulation layers. We are able to separate two different L-H interface improvements.

- one is directly related to the electric field created near the surface [29,$4 \div 6$] or inside the silicon single-crystal as well as inside the inserted complex interface. This field can be appreciably greater than the one of the P-N junction space–charge if a complex interface is formed inside this space-charge (but the complex interface is not necessarily situated at the emitter).
- another concerns the recombination mechanisms inside the L-H accumulation layer. The L-H interface acts at first on the low-side ajority carrier distribution (unipolar theory) [29]. The results published in [6] suggest that the L-H interface causes an excess minority carrier distribution in the front face and that its distribution differs significantly from the simple exponential profile that occurs in a conventional cell structure.

Design of a model BSF cell. The above ideas have allowed a new design of solar cell of the L-H multi-interface type. This design is based on a typical BSF (n^+-p-p^+) configuration where the total device thickness can be strongly reduced down to 5 μm. Two shallow junctions (P-N and L-H) can be formed at sub-μm depth, e.g. $0.2 \div 0.5$ μm [35]. The limitation on single-cell efficiency arises principally because the range of photon energies covered by the solar spectrum is too broad for efficient conversion by a single material [36]. Thus solar photons with energies less than the band-gap cannot generate electron-hole pairs.

A remedy exists in a sub-structure equipped at its front and back edges with two L-H type interfaces [$4 \div 7$]. This fine sub-structure consists of a strongly modified silicon material (empty cavities, defects, very large impurity density, structural deformations, another material, etc.) forming a *complex interface*. The inserted sub-structure can play a similar role as the silicon tandem cell [36] but with improvements of the whole systems electronic transport characteristics (especially the minority carrier lifetime and diffusion length) and optical conversion (without losses in a filter or reflector).

A simple recombination model which agrees with experiment has provided useful design rules for BSF solar cells. The analysis indicates that an optimum structure consists of a passive surface and a thin p^+ region with constant doping in the mid-10^{18} range. The magnitude of the back field is not very critical [23,36]. To be able to improve BSF cell performance it is necessary to proceed by modifying solar cell sub-structure materials to give them special optical properties. Without this the L-H interface improvement is not particularly noteworthy.

Light trapping. The desired optical confinement allows a reduction in width of the *active sub-region* [18]. Local light intensity in a medium with textured and inhomogeneous optical sheets will tend to be $2 \times n(x) \approx 25$ times greater (for crystalline silicon) than the externally incident light intensity. Here $n(x)$ is the local one-dimensional index of refraction in the sheet. One can expect that this condition will be surpassed in a new multi-interface structure. Our infrared light trapping condition necessitates hundreds of reflections.

Absorption. In previous simulations, every absorbed photon produced an electron – hole pair (light absorption by free carriers was totally neglected). Reduction of the band-gap by the heavy doping effect was not considered. All absorption data bases necessary for simulations were created by parameter

modifications. To compare the L-H interface effect a comparison of cells with and without δ-doping sub-structure of the same optical absorption has been adopted.

A model structure was based on a typical BSF configuration (n^+-p-p^+) of 200 μm thickness with two shallow junctions (P-N of 0.5 m and L-H of 3.0 μm). If the *surface recombination velocity* is smaller than the *diffusion velocity* s_{diff}, the *effective recombination velocity* can be made even smaller than the minimum s_{diff} by reducing the width of the p^+ region. The p^+ region thickness (3.0 μm) is overestimated in our cell design to avoid a contact influence. The improved results can be obtained with a p^+ thickness ranging from 0.2 μm up to 1 μm, and a back surface concentration ranging from 5×10^{18} cm^{-3} up to 3×10^{19} cm^{-3}

Modeling and simulation demonstrated that a considerable increase in silicon single-crystal BSF solar cell performance is possible by emitter modifications to give a δ-BSF device. To be efficient, optical and electronic improvements have to act simultaneously in a completely built device because of interactions on the material and device levels.

6. Towards a δ-BSF device realization

First experimental approaches, reported in [7,20,21], have been realized on simplified δ-BSF devices, where in the case of the most developed structure, only emitter with inserted sub-structure, the base (with and without BSF) and contacts were present.

Crystalline structure and doping profile. In a simplified device, the realization the absorbing sub-structures (see Figs. 7 and 8) has been formed by phosphorus ion implantation at $\approx$180 keV and subsequent thermal treatment [7,20,21] as a buried continuous planar nanostructure. An amorphous layer 70 nm thick was placed below a single-crystal layer of 97.5 nm (see Figs. 8$\div$10). The modified material has a large doping concentration which in practice is totally ionized. The doping profile and the active doping profile have been measured respectively by SIMS and spreading resistance methods (Fig. 9).

In Fig. 3 are shown theoretical and experimental (doping and free carrier) distributions: random (simulated) and channeling (experimental) implantation distributions in comparison with the free carrier random distribution (experimental). The sub-structure evolution in thermal treatment is visualized. Only in the region under the sub-structure is a part of the implanted impurity electrically neutral.

Optical improvement. The measurements of optical properties, i.e. reflection, transmission and absorption, were carried out on the simplified devices having only the base and multi-interface emitter [1,7]. Fig. 6 shows the spectral distribution of the optical absorption measured on a simplified device by photothermal deflection spectroscopy (PDS) in comparison with single-crystal silicon bulk characteristics. An amorphous silicon absorption is reported in Fig. 4. In this experiment the widened optical absorption has been observed in a device without any external light trapping up to λ = 2500 nm ($h\nu\approx$0.5 eV) at the relatively constant level of $\alpha\geqslant10^2$ cm^{-1} which is the best result published to date.

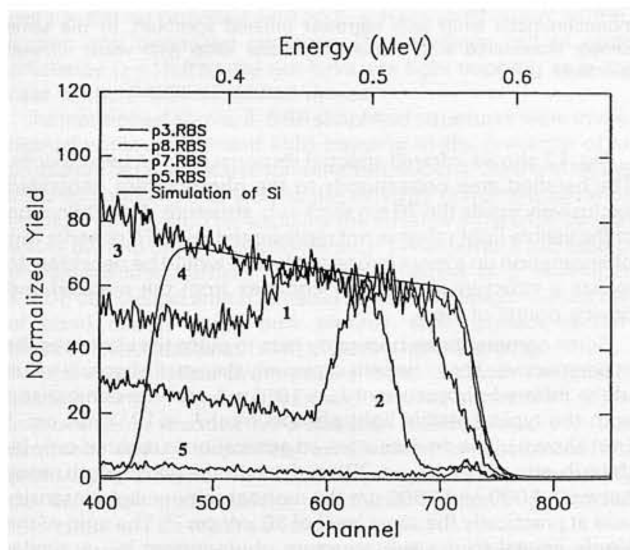

Fig. 8. Structural composition of a phosphorus implanted emitter visualized by Rutherford backscattering (RBS): curve (1) – the as-implanted distribution, curve (2) – final distribution after thermal treatment, curve (3) – a reference distribution for single-crystal silicon, curve (4) – a reference distribution for amorphous silicon and curve (5) simulation of a silicon amorphous layer. The obtained sub-structure has a thickness of d = 70 nm at the depth x_Δ = 97.5 nm. The P-N interface is inserted at the depth x_j = 0.5 μm from the front face [7,20,21]

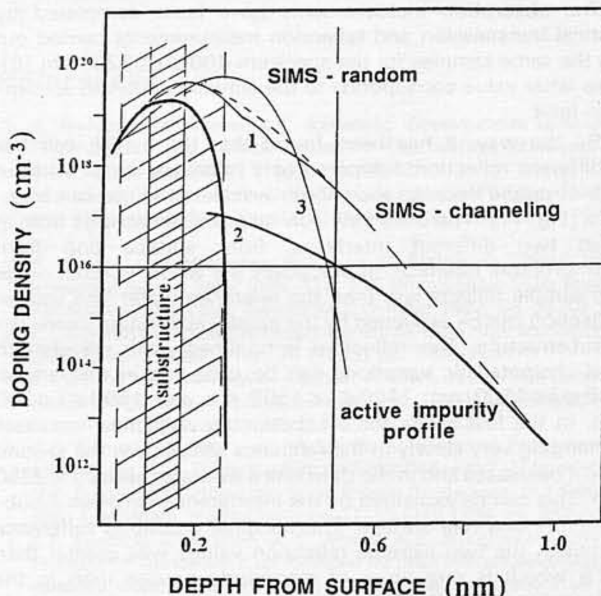

Fig. 9. Comparison of three distributions in a phosphorus implanted sample by channeling: 1) experimental profile by SIMS, 2) two experimental spreading resistance profiles (active impurities), 3) theoretical profile of random atomic impurities [20, 21]

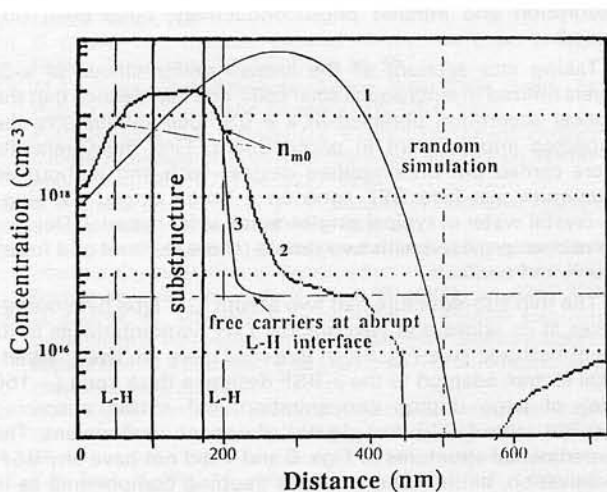

Fig. 10. Comparison of three distributions: 1) theoretical distribution of random-implanted atomic impurities, 2) experimental distribution of free carriers by channeling-implantation (spreading resistance profile) and 3) theoretical distribution of free carriers around an abrupt L-H interface [20, 21]

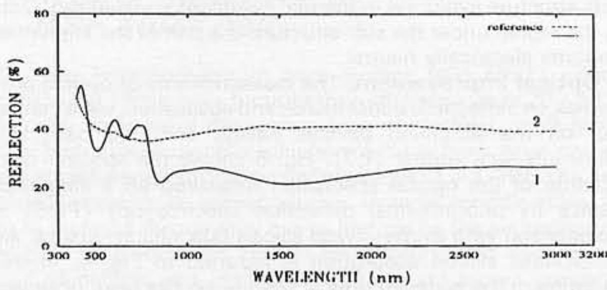

Fig. 11. Comparison of front polished surface reflection: curve (1) samples of Figs. 8÷10 and curve (2) – corresponding non-treated single-crystal wafer [21]

The absorption measurements have been completed by optical transmission and reflection measurements carried out on the same samples for the spectrum $400 \leqslant \lambda \leqslant 3200$ nm [6]. This latter value corresponds to the actually observed absorption limit.

By the way, it has been found that the δ-BSF cell has a different reflection compared to a reference wafer without sub-structure because the shorter wavelength light can interfere (Fig. 11). There are new sub-structure reflections from at least two different interfaces: front surface and front sub-structure interface. In practically the whole infrared range the sample reflects less than the reference wafer The smaller reflection can be explained by the greater absorption inside the δ-substructure. This reflection is nonlinear with wavelength and characteristic variations can be observed in the ranges: $840 \leqslant \lambda \leqslant 1100$ nm, $1100 \leqslant \lambda \leqslant 1500$ nm and $1500 \leqslant \lambda \leqslant 300$ nm. In the first range the δ-substructure reflection increases (changing very slowly in the reference sample), in the second one it decreases and in the third one it saturates above $\lambda \approx 2250$ nm. This can be explained by the interference between δ-substructure and rear surface. The maximal measured difference between the two extreme reflection values was greater than 12% which is one order of magnitude greater than in the reference sample. On the basis of these results we can conclude that the infrared absorption has been widened in our δ-BSF simplified cell up to 3200 nm.

Infrared photocurrent. Measurements of optical absorption and carrier photogeneration were carried out on the same samples but at different technological stages. Simultaneous improvements in both fundamental features, the widened absorption and infrared photoconductivity, have been obtained.

Taking into account all the known performances of α-Si layers utilized in amorphous solar cells, one can deduce that the optical absorption obtained in a δ-BSF cell should give the expected improvement in photocurrent. First measurements were carried out on simplified devices with and without an aluminum rear-face BSF zone on a boron doped CZ single-crystal wafer of typical single-crystal solar material. Devices have been provided with two simple (sheet rear and grid front) aluminum contacts.

The thin sub-structure had two abrupt L-H type heterointerfaces at its edges and two gradual L-H homointerfaces in its neighborhood (see Fig. 9). In this case there are two geometrical factors adapted to the δ-BSF design: a thick zone ($\sim$150 nm) of large doping concentration and a thin absorbing sub-structure ($\sim$70 nm) devoid of optical confinement. The experimental structures of Figs. 6 and 7 did not have any BSF, passivation, antireflection or light trapping components as in our previous absorption investigations. The same infrared photogeneration and photoconductivity measurements have been carried out on a reference solar cell from a similar CZ single-crystal solar material. This reference device of a relatively good efficiency (η=15.8%) was fabricated in the Fraunhofer Institute as a totally finished cell.

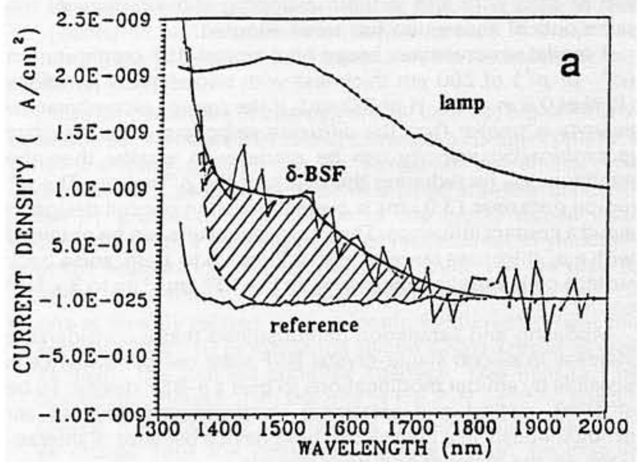

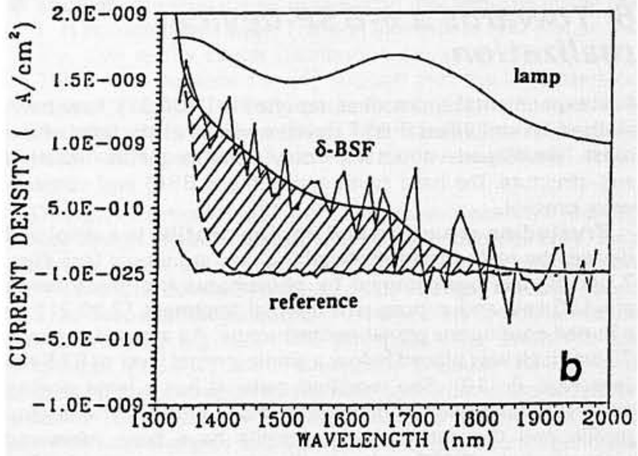

Fig. 12. Infrared photocurrent in silicon single junction single-crystal devices as a function of wavelength [21]. The measurements have been carried out on δ-BSF simplified experimental and on complete reference devices: reference device of efficiency $\eta = 15.8\%$ from the Fraunhofer Institute (Freiburg). Curves concern: a) the sample illuminated with the monochromator lamp with narrower infrared spectrum, b) the same sample illuminated with a monochromator lamp with wider infrared spectrum

Fig. 12 shows infrared spectral responses of the two devices. The hatched area corresponds to the photocurrent generated exclusively inside the 70 nm thick sub-structure. A modification in the visible light range is not represented here. To observe this phenomenon on a more important level it would be necessary to realize a structure sufficiently complex from the material and device points of view.

Some comments are necessary here to place the above results in perspective. They concern especially the small absolute value of the infrared photocurrent $I_{inf} \approx 10^{-9}$ mA cm^{-2} in comparison with the typical visible light photocurrent $I_{inf} \approx 10^{-5}$ mA cm^{-2} (not shown). The devices infrared generation is realized only by the sub-structure of $d_{sub} = 70$ nm thick. In the wavelength range between 1000 and 1600 nm the monochromatic light intensity was at practically the same level of 30 μW cm^{-2}. The ratio of the single-crystal to the sub-structure photocurrent is . A similar value concerns the single-crystal and sub-structure thickness ratio with the absorption coefficient in both cases $\alpha \approx 10^2$ cm^{-1} corresponding to the fundamental absorption at $\lambda \approx 1000$ nm and a range of infrared absorption $\lambda \approx 1000$ to 2500 nm. If we neglect other phenomena, the (1-1/e) part of the incident light is absorbed on a 271 μm path (the complete cell was 350 μm thick). This is $\approx 10^4$ times greater than the sub– structure thickness!

7. Discussion and concluding remarks

The above results show that there is a realistic basis for a conversion efficiency improvement up to 35÷40% at AM1.5 G and non-concentrated light for single-crystal silicon solar cells. It requires a multi-interface design and the incorporation of known device improvements such as widened *local absorption* and *light trapping* together with the built-in electric field. This analysis has proceeded through a systematic design cycle to achieve a projected silicon solar cell morphology that exhibits more than a 35% power conversion efficiency.

The considerations began with a simulation of todays conventional BSF cell. Results were examined and the most logical or practical modifications, including the use of an L-H interface electric field and recombination modifications, that effect improvement have been identified. This approach was continued through succeeding analyses until a cell with efficiency $\eta \geqslant 40\%$ was theoretically defined. To compare, the highest AM1 one-sun efficiency in two-cell tandem structures is expected to be 36÷37% [36]. The cell with an inserted sub-structure can do a few percent better. However the L-H interface cell necessitates substantial fabrication improvements in *absorption and light trapping properties*.

It has been demonstrated that the modified δ-BSF cell emitter can possess simultaneously the necessary structural, optical and electronic properties. To fabricate such silicon cells, much better understanding of material properties and cell structures must come about before the technological advance can be made. One of the possible experimental approaches consists of doping impurity implantation and thermal treatment. This processing allows the formation of a sub-structure (in the form of a complex interface) buried below a single-crystal layer. It signifies that the locally modified crystalline material (up to amorphization) is contained between homo– or heterointerfaces as a planar continuous nanostructure.

This sub-structure should have the infrared optical absorption up to 3200 nm as could be observed in PDS, transmission and reflection measurements on a simplified δ-BSF device (absorption coefficient $\beta \geqslant 10^2\ cm^{-1}$). The corresponding infrared photocurrent has been measured at a relatively important level in the range $1100 \leqslant \lambda \leqslant 1900$ nm, e.g. up to the upper lamp flux limit. The δ-BSF infrared current variation has been compared with that of a finished classical single-crystal thick cell (>250 m) provided with BSF, surface passivation, antireflection and optimized contacts. The reference cell of good efficiency (η=15.8%) did not have any light trapping as in the case of the δ-BSF simplified device.

As mentioned above, δ-BSF simplified structures were investigated without BSF and light trapping in the presence of an unusually large surface recombination velocity. So the effective infrared generation as well as the minority concentration were strongly disturbed. This explains the so large difference between visible and infrared photocurrents. An important increase of photogenerated carriers should be obtained in a developed δ-BSF cell design which consists of a silicon single-crystal cell of good quality (long bulk lifetime, small surface recombination) and equipped with effective light trapping.

Now it is possible to propose a multi-interface cell design based on single– crystal silicon with infrared conversion. Other improvements founded on a complex interface insertion that combines several separately investigated or postulated improvements are possible. Some important results concerning the increased photocurrent, electronic transport and carrier collection will be reponed later.

The future fabrication of a silicon single junction device for non-concentrated light would necessitate uniting recent technological advances in the sub-structure and the total device to ensure the: i) widened optical absorption by low energy photon absorption, ii) optical confinement of light non-absorbed in one pass, and iii) formation of the L-H type interfaces at its edges.

This new design will allow a future development of very promising devices being able to compete with classical energy sources with resulting multiple consequences on all levels of society. It seems that photovoltaic conversion can give the desired solution but a technological stimulation on the highest level is needed.

Acknowledgments

The author wishes to express his thanks to Dr J.-C. Muller of the Laboratory PHASE for his comments, and to Dr. M. Lipinski of the Experimental Solar Energy Station of the Polish Academy of Science for his help in the simulation of the devices investigated to Dr. U. Zammit of the Universita di Roma (Italy) for his PDS measurements, to Dr R. Schindler from the Fraunhofer Institute of Freiburg (Germany) for the reference cell, to E. Andre of CNET-CNS Meylan (France) for his spreading resistance measurements and to researchers from the PHASE Laboratory of Strasbourg (France): Dr J.-J. Grob, A. Grob and Y. Le Gall for implantations and RBS characterizations, Dr R. Stuck for his SIMS measurements, and Dr J.-P. Ponpon, L. Ventura, J.-P. Schunck, and H.E. Strazynska-Kuznicki for their experimental aid.

References

1. *A. Rohatgi, E.R. Weber, L.C. Kimerling*: Opportunities in Silicon Photovoltaics and Defect Control in Photovoltaic Materials. J. Eectronics Materials, **22** (1993) pp. 65-72.
2. *M.A. Green*: Silicon Solar Cells: Evolution, High-Efficiency Design and Efficiency Enhancements. Semicond. Sci. Technol., **8** (1993) pp. 1-12.
3. *R. Swanson, P. Verlinden, R. Crane, R. Sinton, C. Tilford*: High Efficiency Silicon Solar Cells. 11th E.C. Photovoltaic Solar Energy Conference, Montreux, Switzerland, October 1992, pp. 35-40.
4. *Z.T. Kuznicki*: L-H Interface Improvement for Ultra High Efficiency Si Solar Cells. J. Appl. Phys., **74** (1993) pp. 2058-2063.
5. *Z.T. Kuznicki, J.C. Muller, M. Lipinski*: A New L-H Interface Concept for Very High Efficiency Silicon Solar Cells. 23rd IEEE Photovoltaic Spec. Conf., Louisville, USA, (1993), pp. 327-331.
6. *Z.T. Kuznicki, L. Wu, J.C. Muller*: Some Electrical Properties of a New Very High Efficiency Silicon Solar Cell with L-H Interfaces. l2th European Photovoltaic Solar Energy Conference and Exhibition, Amsterdam, the Netherlands, 11-15 April 1994, pp. 552-555.
7. *Z.T. Kuznicki, J.-J. Grob, J.-C. Muller, H.E. Strazynska-Kuznicki*: Procédé de fabrication d'un matériau ou dispositif photovoltaique, matériau dispositif ainsi obtenu et photopile comprenant un tel materiau ou dispositif. French patent pending No 94 08885 from 13 July 1994.
8. *Z.T Kuznicki and collaborators*: Rapport Annuel d'Activité du Groupe: "Nouvelles structures semiconductrices pour application aux photopiles" du Laboratoire PHASE. III Etude préliminaire sur une sub-structure absorbante de la cellule solaire δ-BSF au silicium monocristallin. Strasbourg, 1994.
9. *P.A. Basore*: PC-ID Instalation Manual and User's Guide Version 3, Sandia Report 1991.
10. *G. Guttler, H.J. Queisser*: Impurity Photovoltaic Effect in Silicon. Energy Conversion, **10** (1970) pp. 51-55.
11. *M.A. Green*: High Efficiency Silicon Solar Cells. Trans. Tech. Publications, Switzerland-Germany– UK-USA, 1987.
12. *P.J. Zanzucchi, C.R. Wronski, D.E. Carlson*: Optical and Photoconductive Properties of Discharge-Produced Amorphous Silicon. J. Appl. Phys., **48** (1977) pp. 5227-5236.
13. *S. Romani, J.H. Evans*: Platelet Defects in Hydroden Implanted Silicon. Nucl. Inst. Meth., **B 44** (1990) pp. 313-311.
14. *U. Zammit, M. Marinelli, R. Pizzoferrato*: Surface States and Buried Interface States Studies in Semiconductors by Photothermal Deflection Spectroscopy. J. Appl. Phys., **69** (1991) pp. 3286-3290.
15. *U. Zammit, M. Marinelli, R. Pizzoferrato, E. Mercuri*: Gap-States Distribution of Ion-Implanted Si and GaAs from Subgap Absorption Measurements. Phys. Rev., B **46** (1992) pp. 7515-7518 and private communication (1994).
16. *M.A. Green*: Crystalline and Polycrystalline Silicon Tandem Junction Solar Cells, Theoretical Advantages. Solar Cells, **18** (1986) pp. 31-40.
17. *Y.S. Tsuo, X. Wu, J.L. Alleman, X. Li, Y. Qu, T. F. Ciszek, R.E. Hollinsworth, P.K. Bhat*: Solar Cell Structures Combining Amorphous, Microcrystalline and Single-crystalline Silicon. 23th IEEE Photovoltaic Spec. Conf., Louisville, USA, May 10-14, 1993, pp. 281-285.
18. *E. Yablonovitch, G.D. Cody*: Intensity Enhancement in Textured Optical Sheets for Solar Cells. IEEE Trans. Electron. Dev., **ED-29** (1982) pp. 300-305.

19. *M. Spitzer, J. Shewchun, E.S. Vera, J.J. Loferski*: Ultra High Efficiency Thin Silicon P-N Junction Solar Cells Using Reflecting Surfaces. l4th IEEE Photovoltaic Spec. Conf., 1980, pp. 375-380.
20. *Z.T. Kuznicki, L. Wu, J.-J. Grob, L. Ventura*: Infrared Absorption of a New Very High Efficiency Si Solar Cell. l2th European Photovoltaic Solar Energy Conference and Exhibition, Amsterdam, the Netherlands, 11-15 April 1994, pp. 1056-1059.
21. *Z.T. Kuznicki, L. Wu, J.-J. Grob, J.C. Muller*: Towards Realization of a -BSF Solar Cell. World Conference on Photovoltaic Energy Conversion (WCPEC), Hawaii, USA, 5-9.12.1994.
22. *J. Mandelkorn, J.H. Lamneck Jr*: Simplified Fabrication of Back Surface Electric Field Silicon Cells and Novel Characteristics of such Cells. Solar Cells, **29** (1990) pp. 121-130: 9th IEEE Photovoltaic Spec. Conf., 1972, pp 66-72.
23. *A. Rohatgi, P. Rai-Choudhury*: Design Fabrication, and Analysis of 17-18-Percent Efficient Surface-Passivated Silicon Solar Cells. IEEE Trans. Electron Dev., **ED-31** (1984) pp. 596-601.
24. *W. Zimmermann*: Measurement of Spatial Variations of the Carrier Lifetime in Silicon Power Devices. Phys. Stat. Sol., (a) **12** (1972) pp. 671-678.
25. *J.G. Fossum*: Physical Operation of Back-Surface-Field Silicon Solar Cells. IEEE Trans. Electron Dev., **ED-24** (1977) pp. 322-325.
26. *M.P. Godlewski, C.R. Baraona, H.W. Brandhorst, Jr.*: Low-High Junction Theory Applied to Solar Cells. Solar Cells, **29** (1990) pp. 131-150; 10th IEEE Photovoltaic Spec. Conf., 1973, pp. 40-49.
27. *P.A. Iles, S.I. Soclof*: Effect of Impurity Doping Concentration on Solar Cell Output. 11th IEEE Photovoltaic Spec. Conf., 1975, pp. 19-24.
28. *F.A. Lindholm, A. Neugroschel, S.C. Pao, J.G. Fossum, C.T. Sah*: Design Considerations for Silicon HLE Solar Cells. 13th IEEE Photovoltaic Spec. Conf., June 5-8, 1978. pp. 1300-1305.
29. *Z.T. Kuznicki*: The Electrical Structure of the Step L-H Junction. **Part I** – Analytical Methods – Physical Background. Electron Technology, **12**, No 2 (1979) pp. 15-35 and **Part II** Electrostatic Problem of the L-H Homojunction. Electron Technology **12**, No 3 (1979) pp. 89-100.
30. *Z.T. Kuznicki*: Electrical Properties of Thin Polycrystalline Films. PWN Warszawa-Lodz, 1984 and Z.T. Kuznicki: Electric Properties of a Finite L-H Junction. Bulletin de l'Académie Polonaise des Sciences Serie des Sciences Techniques, **34**, No 3-4 (1986) pp. 225-233.
31. *Z.T. Kuznicki*: Low-High Homojunction in the Stationary State. J. Appl. Phys., **69** (1991) pp. 6526-6541.
32. *M. Wolf*: Drift Fields in Photovoltaic Solar Energy Converter Cells. Proc. IEEE, (1963) pp. 674-693.
33. *J.G. Fossum, E.L. Burgess*: High-Efficiency p^+-n-n^+ Back-Surface -Field Silicon Solar Cells. Appl. Phys. Lett., **33** (1978) 238-240.
34. *T.I. Chappell*: A Study of the Conversion Efficiency Limit of p^+ -i–n^+ Silicon Solar Cells in Concentrated Sunlight. IEEE Trans. Electron. Dev., **ED-21** (1980) pp. 760-766.
35. *J. Michel, A. Mircea, E. Fabre*: Computer Analysis of Back-Surface Field Silicon Solar Cells. J. Appl. Phys., **46** (1975) pp. 5043-5045.
36. *J.C.C. Fan*: Single-cell Concept for Obtaining Photovoltaic Conversion Efficiency over 30%. 18th IEEE Photovoltaic Spec. Conf., 1985, pp. 28-32.